

Effect of Coconut Fiber and Ground Granulated Blast Furnace Slag on the Flexural Strength, Toughness and Deformation of Foamed Concrete

Jun Huang^{1,2,3,4,*}, Shichun Qiu¹, and Denis Rodrigue⁵

¹College of Civil Engineering and Architecture, Wenzhou University, Wenzhou, China

²Key Laboratory of Engineering and Technology for Soft Soil Foundation and Tideland Reclamation of Zhejiang Province, Wenzhou, China

³Wenzhou Engineering Technical Research Center on Building Energy Conservation and Emission Reduction & Disaster Prevention and Mitigation, Wenzhou, Zhejiang, China

⁴Zhejiang Collaborative Innovation Center of Tideland Reclamation and Ecological Protection, Wenzhou, Zhejiang, China

⁵Department of Chemical Engineering, Laval University, Quebec, Canada

Abstract: To reduce environmental pollution and decrease cement consumption, ground granulated blast furnace slag (GGBS) was used as a partial replacement (10 wt.%) to produce foamed concrete. The results showed that GGBS addition did not significantly modify the flexural strength of foamed concrete, but increased its brittleness, reducing deformation at peak load by 70%. To improve these properties, coconut fibers were added (up to 0.5 vol.%) leading to higher mechanical strength and toughness. Based on the flexural strength of foamed concrete, the optimal fiber content was 0.4 vol.% depending if GGBS was added (improvement 21.3%) or not (16.7%). Coconut fibers were also found to improve the flexural toughness by two to three times compared to neat foamed concrete with or without GGBS at 2 mm of deflection. To get more information on the flexural behavior, strain gauges were used to measure the axial and transverse strains, clearly showing the positive role of coconut fiber addition on improving the mechanical properties of foamed concrete, especially for the strain energy densities. Finally, scanning electron microscopy (SEM) was used to analyze the samples morphology and explain the mechanical results.

Keywords: Foamed concrete, Coconut fiber, Ground granulated blast furnace slag, Flexural properties, Microstructure.

1. INTRODUCTION

As a lightweight, eco-friendly and low energy consumption material, foamed concrete was developed to produce excellent physical and mechanical properties. Due to its functional characteristics (low density and thermal conductivity with fire resistance), foam concrete is now widely used in several civil engineering applications, such as sound insulation, photocatalytic technology [1], wall thermal insulation [2], thermal energy storage [3], and fire insulation [4]. Due to its lightweight combined with non- and semi-structural characteristics, foamed concrete can also be used as backfilling material for abandoned urban underground spaces [5], as well as energy absorption material for high geo-stress soft rock tunnels [6]. Although cellular concrete was first patented by Bayer and Eriksson in 1923 [7], and comprehensively reviewed for its physical properties by Rudolph *et al.* in 1954 [8, 9], foamed concrete was used in construction applications as a lightweight material which has substantially increased over the last twenty years. Based on its energy efficient nature and potential sustainability features, a great deal of interest

was devoted to improve the physical and mechanical properties of foamed concrete by optimizing its components and micro-structure. For example, if Portland cement can be partially replaced by sulphoaluminate cement, the bubble diameter of the fresh foamed concrete can be reduced for 3D printed samples [10]. This is important to reduce the amount of energy consumed and limit environmental pollution, as a portion of cement can be replaced by silt to make foamed concrete. Replacing a portion of cement with silt has been shown that the volume strain of the specimen increased with increasing silt content [11]. Furthermore, when Portland cement was completely replaced by other active mixtures, such as fly ash and silica fume, foamed geopolymer concrete was produced. Because of their low density, cenospheres are also good substitutes instead of fly ash to generate ultra-lightweight foamed geopolymer concrete [12]. Using a heat treatment, polyethylene powder was shown to have a similar role leading to even smaller effective pore sizes inside the foamed concrete [13]. When expanded perlite was used to replace sand, a fine and regular pore size distribution was obtained [14]. Bottom ash and limestone can also be used as aggregates to prepare foamed concrete. It was reported that adding bottom ash substantially lowered the thermal conductivity (0.633 W/m·K) compared to

*Address correspondence to this author at the College of Civil Engineering and Architecture, Wenzhou University, Wenzhou, China; Tel: +86 13587607056; E-mail: junhd@wzu.edu.cn

limestone (0.795 W/m·K) [15]. In addition, other reinforcements, such as inorganic ferrous–ferric oxide nanoparticles [16], and hydroxypropyl methylcellulose [17], were both investigated to improve the durability and rheological properties of foamed concrete.

In general, the mechanical properties of foamed concrete are mainly controlled by the morphology (formulation and dispersion) and cell sizes distribution. For the latter, different foaming agents can be used to create the voids (cellular structure) [18]. But foamed concrete with different superabsorbent polymers (crosslinked poly sodium acrylate) exhibited higher foam stability and generated a more homogeneous pore structure [19]. For the stabilization of high-performance foamed concrete, a detailed review was conducted recently [20].

As an industrial by-product or solid waste, ground granulated blast furnace slag (GGBS) is considered to be a potential viable active substance in the development of eco-friendly foamed concrete. This material is composed of different oxides such as CaO, SiO₂, and Al₂O₃. Previous studies showed that GGBS can decrease the heat of hydration, reduce environmental pollution, and improve the mechanical properties of foamed concrete [21]. With a maximum size of 4 mm, foamed concrete based on 100% GGBS exhibited a lower bulk density, ultrasound velocity, and thermal conductivity, as well as higher compressive strength than the control specimens [22]. With a median diameter of 4.254 µm for the ultrafine slag, significant improvement in compressive strength (11%) and the ratio of strength over density (6%) of foamed concrete was reported after 28 days [23].

The production of Portland cement is well-known to consume high amounts of energy and emits a large amount of CO₂. So the use of alkali-activated slag and generating a cellular structure can both decrease the consumption of Portland cement as well as producing higher flexural and compressive strengths than that of ordinary Portland cement foamed concrete [24, 25]. To compare the compatibility of foaming agent and the alkali-activated slag cement, three types of anionic surfactant (AOS, AES, and K12) with the same foam stabilizer were selected as the foaming agent [26]. The results showed that the foaming ability of AOS and AES was better than that of K12, while the foam stability of AOS and K12 was slightly better than that of AES. Although alkali-activated slag cement can save energy and indirectly protect the environment, strong alkalis, such as NaOH and NaSiO₃, can also lead to fast setting, high cost and the risk of environmental contamination. But calcium hydroxide was shown to be a good alternative to alkaline solutions, which can be obtained from carbide slag (another solid waste) to activate granulated blast furnace slag [27].

Foamed concrete has several advantages such as better thermal insulation and fire resistance. However, it has lower mechanical strengths because of high porosity. To enhance the mechanical behavior of foamed concrete, short fibers are often randomly distributed in the cementitious matrix during the mixing stage. With their bridging role (reduce crack propagation), a wide variety of different fibers, including glass [28, 29], polypropylene (PP) [30, 31], recycled polyethylene terephthalate (PET) [32], basalt [33], and polyvinyl alcohol (PVOH) [34] were reported to improve the mechanical strength of foamed concrete. But compared with these synthetic fibers, natural (biosourced/lignocellulosic) fibers are more environmental friendly, inexpensive, biodegradable, and renewable. They can also improve the mechanical properties of foamed concrete. For example, combining 10 wt.% of fly ash and hemp fibers in foamed concrete generated high flexural strength at 50 and 75 kg/m³ [35]. When sisal fiber was used, its optimal volume fraction was 0.133% [36, 37]. A similar work conducted by Raj *et al.* showed that the optimal total fiber volume fraction was 0.3% to get the maximum strength when coir and PVOH fibers were used together [38].

As a waste materials produced by the coconut husk, coconut fiber is eco-friendly and low cost produced in hot and wet tropical regions. The production of coconut fruit is estimated at 60 million tons every year [39], leading to a high amount of residues after processing. So the fibers extracted can be used as reinforcement in composite structures. For example, the addition of coconut fibers was shown to improve several properties of cement based composites, such as strength [40, 41], toughness [42, 43], shrinkage [44], durability [45], and dynamic properties [46, 47]. Nevertheless, wetting and drying cycles can result in fiber breakup and debonding from the matrix leading to lower mechanical strength of cementitious composites [48]. In fact, the bonding strength between coconut fibers and the cement matrix is known to be affected by the fiber sizes (diameter and length) and the concrete formulation (components and concentration) [49]. To modify the interfacial adhesion, coconut fibers were pretreated by a solution of NaOH and H₂O₂ to improve the damping properties of the composites [50]. Ahmad *et al.* [51] also investigated the effect of coconut fiber length and content on the properties of high strength concrete. The results showed that the optimal coconut fiber length and content were 50 mm and 1.5 wt.%, for which the flexural strength and corresponding toughness index increased by 3% and 94%, respectively. Under flexion, the total energy absorption was improved by up to 162% compared to the neat high strength concrete.

Although coconut fibers are widely used in civil engineering because of their numerous advantages, it is not clear if coconut fibers can improve the mechanical properties of foamed concrete. In our previous studies [36, 52], sisal fibers were added into foamed concrete to determine their effect on the mechanical properties and fatigue life of cement based composites. In this study, ground granulated blast furnace slag is combined with coconut fibers to enhance the mechanical properties of foamed concrete with a focus on toughness and strength.

2. MATERIALS AND METHODS

2.1. Raw Materials

The raw materials used in this work include cement, silica fume, sand, water reducer, foaming agent, calcium stearate, slag, coconut fiber, and water. P·O 42.5 was purchased from Yueqing Hailuo cement Co.

Ltd. (Wenzhou city, China) and its technical properties are listed in Table 1. Silica fume was purchased from Longze water purification material Co. Ltd. (Gongyi city, China) with a small particle size and large specific surface area as it can restrain the reaction between alkali and aggregate to prevent the propagation of micro-cracks (Table 2). Ground granulated blast furnace slag (GGBS) was bought from New materials Co. Ltd. (Gongyi city, China) and the main properties are reported in Table 3. The fine sand was obtained from Zhongma mining Co. Ltd. (Wenzhou city, China). H₂O₂ was used as the foaming agent and supplied by Huize bioengineering Co. Ltd. (Henan province, China). The coconut fibers were purchased from Jiagaocheng import and export trade Co. Ltd. (Shang Gao city, China) and their technical characteristics are listed in Table 4. Calcium stearate was used as a foam stabilizer and produced by Baiyilian chemical Co. Ltd. (Hebei province, China) with the parameters listed in Table 5. Polycarboxylate water reducer was selected to

Table 1: Technical Parameters of P·O 42.5

Loss on Ignition (%)	SO ₂ (%)	MgO (%)	Specific Surface Area (m ² /kg)	Setting Time (min)		Cl ⁻ (%)	Soundness
				Initial	Final		
3.21	2.06	1.69	343	182	231	0.033	Qualified

Table 2: Technical Parameters of Silica Fume

Item	Specific Surface Area (m ² /g)	Loss on Ignition (%)	Nitrogen (%)	SiO ₂ (%)	Alkali (%)
Standard	≥ 15	≤ 4	≤ 0.1	≥ 85	≤ 1.5
Testing value	20	1.3	0.004	97.8	0.9

Table 3: Technical Parameters of Ground Granulated Blast Furnace Slag

Item	Activity Index (%)		Density (g/cm ³)	Specific Surface Area (m ² /kg)	Fluidity Ratio (%)
Standard	7 d	28 d	≥ 2.80	≥ 400	≥ 95
	≥ 75	≥ 95			
Testing value	90	99	2.84	472	96

Table 4: Technical Parameters of the Coconut Fibers

Diameter (mm)	Length (mm)	Density (g/cm ³)	Moisture Capacity (%)	Tensile Strength (MPa)	Elastic Modulus (GPa)	Elongation (%)
0.15-0.35	20	1.2	10-12	128-157	3.86-5.6	21.2-40.3

Table 5: Technical Parameters of Calcium Stearate (C₁₇H₃₅COO)₂Ca

Item	Density (g/cm ³)	Melting Point (°C)	Calcium (%)	Free acid (%)	Heat Variation (%)	Fineness (pass 75 μm) (%)
Value	1.08	149-155	12.5±0.5	0.5	≤ 2	99

improve the mixture fluidity and bought from Hongxiang construction additive company (Laiyang city, China). All the materials were used as received.

2.2. Specimen Preparation

2.2.1. Fiber Treatment

The original coconut fiber is rough and includes some impurities on the surface, which will affect the foaming ability and their dispersion. In order to decrease these effects, the coconut fibers should be pre-treated. First, they were soaked in water and washed three times, each time for 30 min. Then, the coconut fibers were placed in an oven (60 °C) for 24 h to remove humidity. Finally, they were cut to 20 mm in length to get good dispersion in the matrix (avoid agglomeration) (Figure 1).

2.2.2. Sample Production

In this study, the coconut fibers were added at six volume fractions including 0.0%, 0.1%, 0.2%, 0.3%, 0.4% and 0.5% with or without (GGBS) to determine their effect on the mechanical properties of the composites. GGBS was added to partially replace cement. The samples were prepared by casting in a

mold having dimensions of 100 mm × 100 mm × 400 mm. The different compositions investigated are listed in Table 6. The design density of the specimen was taken as 1150 kg/m³. All the tests consisted of twelve groups, and each group had three samples with codes. FC-0 refers to a foamed concrete without GGBS and coconut fiber, while FCS-0 represents a foamed concrete with 10 wt.% GGBS. Similarly, FCS-0.5 represents a foamed concrete with 10 wt.% GGBS and 0.5 vol.% coconut fibers.

Each component was weighed by an electronic platform scale which was bought from Baoshan measurement factory (Shanghai, China) with a precision of 0.05 kg. All the molds were cleaned by a brush and coated with an engine oil (#30) to improve demolding. Before the specimens were prepared, the mixer was cleaned by a water gun to remove any residual impurities.

Specimen preparation was composed of several steps. First, weigh the cement, fine sand, silica fume, and GGBS and place in the mixer in this sequence to dry mix for 3 min. Second, manually dispersed the coconut fibers into the mixer and dry mix for 3 min. Third, add the foaming agent and water in the mixer

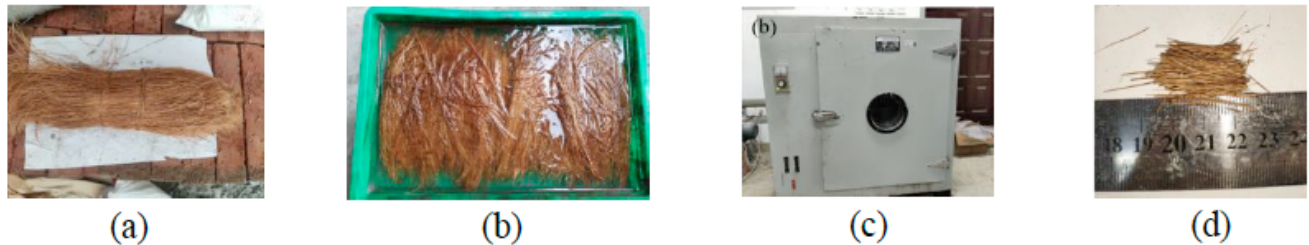


Figure 1: (a) Original coconut fiber; (b) soaking and washing; (c) coconut fiber drying; (d) short coconut fiber (20 mm length).

Table 6: Compositions of the Foamed Concrete Prepared (unit = kg)

Group	Cement	Silica Fume	Sand	H ₂ O ₂	Water Reducer	Calcium Stearate	Water	Slag	Fiber
FC-0	450	45	540	5	1.575	0.9	202.5	0	0
FC-0.1	450	45	540	5	1.575	0.9	202.5	0	1.2
FC-0.2	450	45	540	5	1.575	0.9	202.5	0	2.4
FC-0.3	450	45	540	5	1.575	0.9	202.5	0	3.6
FC-0.4	450	45	540	5	1.575	0.9	202.5	0	4.8
FC-0.5	450	45	540	5	1.575	0.9	202.5	0	6.0
FCS-0	405	45	540	5	1.575	0.9	202.5	45	0
FCS-0.1	405	45	540	5	1.575	0.9	202.5	45	1.2
FCS-0.2	405	45	540	5	1.575	0.9	202.5	45	2.4
FCS-0.3	405	45	540	5	1.575	0.9	202.5	45	3.6
FCS-0.4	405	45	540	5	1.575	0.9	202.5	45	4.8
FCS-0.5	405	45	540	5	1.575	0.9	202.5	45	6.0



Figure 2: Images of the samples prepared.

and wet mix for 2 min. Fourth, add all the other admixtures in the mixer and mix for 30 s. Finally, the stirred cement slurry was poured into the mold and placed on a vibration table for 30 s and then smooth out the surface with a spatula (Figure 2). All the specimens were demolded after two days, and then placed in the laboratory to be cured at room temperature until the corresponding age was reached.

2.3. Mechanical Properties

2.3.1. Four-Point Bending Test

In this study, four-point bending tests were conducted on an electronic universal testing machine (MTS Co. Ltd., China). The span was fixed at 300 mm and the distance between the loading and support points was 100 mm (Figure 3). In order to eliminate any motion and deformation of the support points, a frame structure was fixed to the specimen with bolts. The mid-span deflection of the specimen was measured by LVDT and all the experimental data were acquired with a computer. The experiments were conducted at Wenzhou University (China) following the standard "Fiber reinforced concrete testing method standard"

(CECS13:2009) [53]. Here, a displacement control mode was selected and the loading velocity was 0.05 mm/min.

2.3.2. Strain Measurement

Under four-point bending test, only the central part sustains axial deformation. In order to compare the effect of coconut fibers on the local deformation of foamed concrete, a strain gauge at the top and bottom of the specimen was perpendicularly installed on the surface of the pure bending region to measure the axial strains (Figure 4). The strain gauges were purchased from Guangce electronic Co. Ltd. (Yiyang city, China). Each strain gauge (BX120-20AA-R1-D150) has a size of 20 mm × 4 mm. To ensure accurate data measurement, a polyvinyl chloride film was used to squeeze out the bubbles when the strain gauge was glued at the measurement positions. The strain data collection was conducted by a dynamic or high speed static strain tester produced by Donghua testing technical Co. Ltd. (Jiangsu province, China). For the strain measurement, a quarter bridge wiring method was selected.

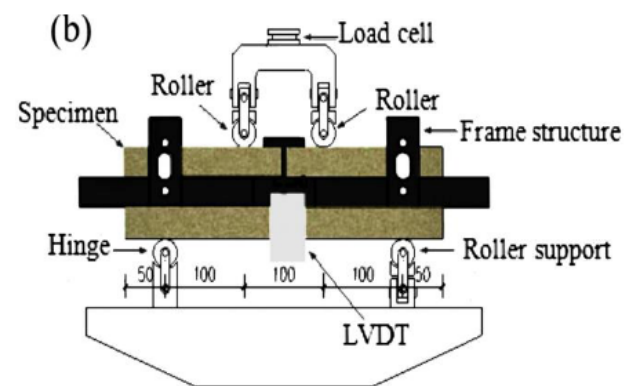
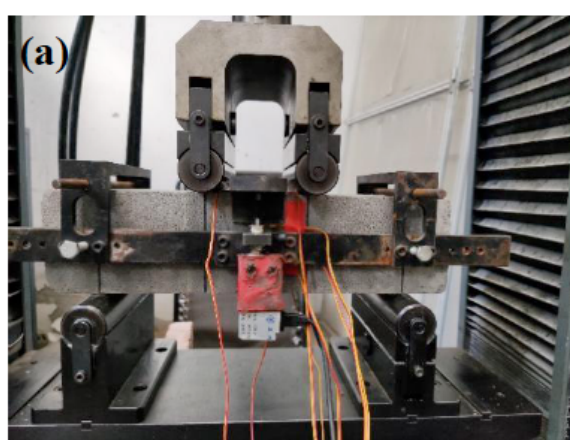


Figure 3: Four-point bending test setup: (a) image of the fixture geometry for bending test and (b) schematic diagram of the set-up. (unit: mm)

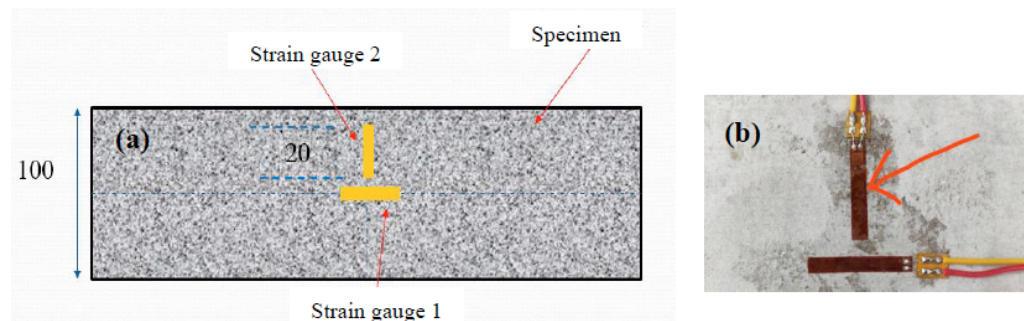


Figure 4: Axial strain measurement: (a) location of the strain gauges and (b) images of the strain gauges. (unit: mm)

3. RESULTS AND DISCUSSION

In order to get the complete flexural load-deflection curves and compare the flexural toughness of foamed concrete with different coconut fiber contents, the external load was applied until a maximum was reached and then decreased to 15% of the peak load. Figure 5(a) shows the failure of a neat foamed concrete (without slag and fiber). It can be seen that this sample has a typical brittle failure and all the cracks extended from the bottom to the top. But with coconut fiber addition, the specimens have much better toughness due to a bridging effect as pulling out or breaking fibers dissipated a high amount of energy. So the specimens gradually revealed a more ductile failure with increasing fiber content. The highest toughness was observed for the sample having the highest fiber content (0.5 vol.%) as the cracks opened at the bottom but did not break (Figure 5b). Figure 5(c) presents a typical example of the fiber bridging effect, while Figure 5(d) reveals the cross-section after specimen failure. Under flexural loading, the specimen is under high

deformation, especially for coconut fiber reinforced foamed concrete. In some cases, the deformation exceeded the strain gauge capacity and broke as presented in Figure (5e).

3.1. Load-Deflection Curves

Figure 6(a) presents typical flexural load-deflection curves of the neat foamed concrete and with 10 wt.% GGBS without coconut fiber. For all these curves, the deflection is small before the load reached a maximum. But when the external load reached the peak value, the deflection rapidly increased. Figure 6(a) (enlargement) shows that GGBS had no significant effect on the strength of the foamed composites. However, when GGBS was added, the deflections related to the peak loads decreased, indicating that GGBS may enhanced rigidity but also the brittleness. By averaging the experimental data, the peak load and the deflection of foamed concrete at 0% and 10 wt.% GGBS were 4.17 and 4.24 kN with 0.04 and 0.012 mm, respectively. The results show that foamed concrete had a higher

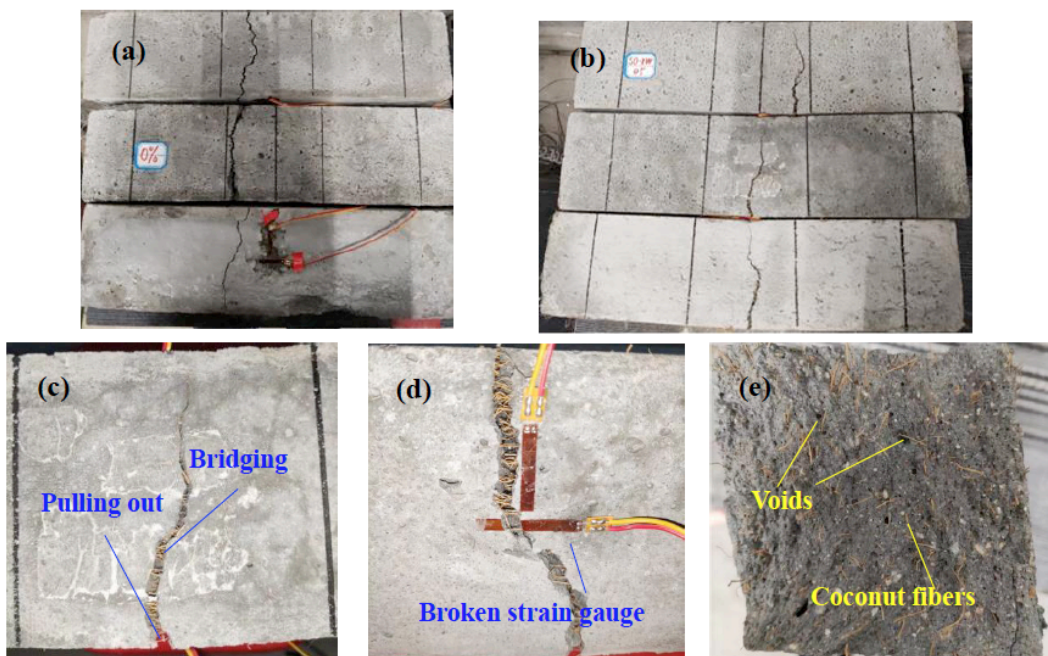


Figure 5: Typical images of failed specimens: (a) neat foam concrete, (b) foam concrete with 0.5% coconut fiber, (c) fiber bridging effect, (d) broken strain gauge, and (e) cross-section of a broken specimen.

strength and a smaller deflection when GGBS partially replaced the cement. When coconut fibers were added, GGBS played a similar role for the peak loads and deflections. With the coconut fibre content increasing, due to the bridging effects of fibres, the deflections of the specimens obviously increased. when the coconut fibre content reached 0.4 and 0.5 vol.% Figure 6(b), the flexural strength of composites also increased. On the other hand, for the two volume fractions of fibers, GGBS not only enhanced the maximum flexural load (0.277 and 0.758 kN), but also increased the deflection (0.047 and 0.023 mm) compared with the specimens with no GGBS. This implies that GGBS and coconut

fiber have a synergistic effect on improving the mechanical properties of these foamed composites.

3.1.1. Piecewise Linear Fitting

From the previous analysis, it was concluded that coconut fibers can affect the strength of composites and significantly improve their toughness. To compare the effects of coconut fibers on the mechanical properties of composites, the experimental data of each group with the same coconut fiber content were fitted. The piecewise linear function can be expressed as the equation (1) and (2), the corresponding fitting parameters for composites with no GGBS were listed Table 7. When coconut fibre volume fraction was taken

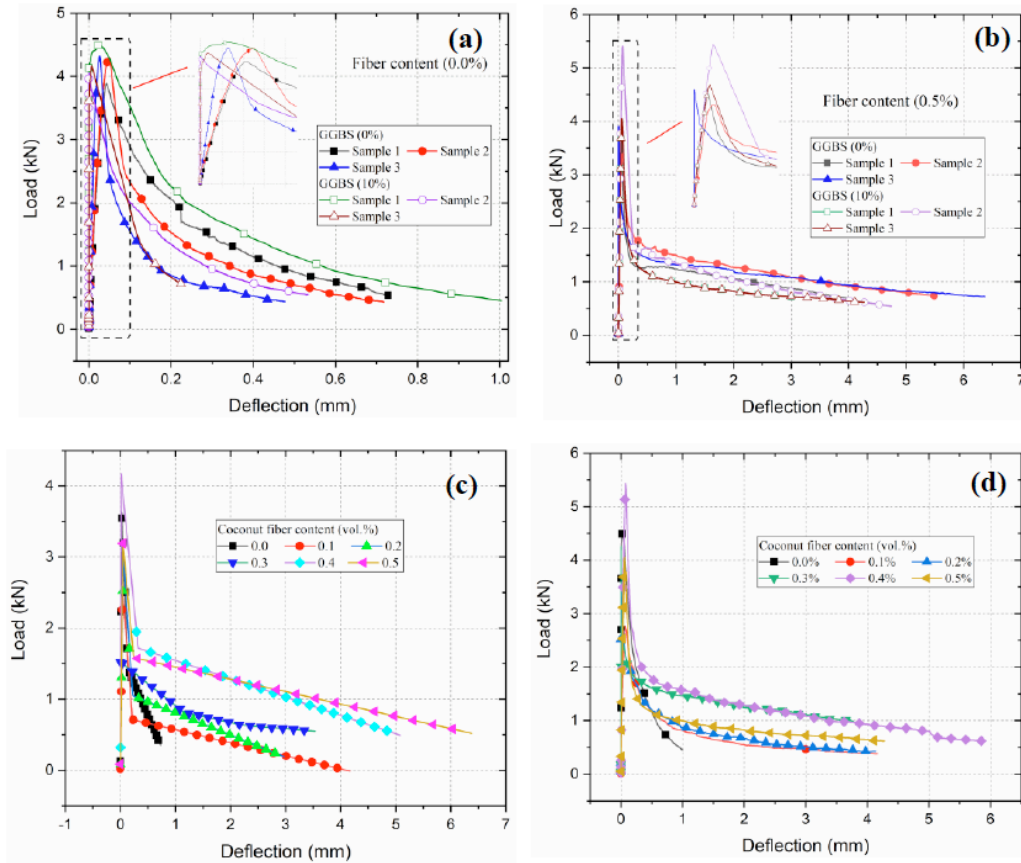


Figure 6: Flexural load-deflection curves of foamed concrete with different volume fraction of coconut fibers: (a) 0.0% and (b) 0.5%; (c) piecewise linear fitting curves, (d) typical flexural load-deflection curves.

Table 7: Piecewise Linear Fitting Parameters

Fiber Content	Fitting Parameters					
	a_1	k_1	x_1	k_2	x_2	k_3
No GGBS	0	0.126	150.370	0.023	-19.351	0.137
	0.1	0.158	67.741	0.036	-10.456	0.215
	0.2	0.147	60.978	0.048	-11.692	0.221
	0.3	1.523	-0.611	1.155	-0.173	2.232
	0.4	0.321	344.439	0.011	-7.989	0.319
	0.5	0.086	69.005	0.045	-8.437	0.236

from 0.0 to 0.5% and GGBS content was 0, the fitting results were plotted in Figure 6(c), from the figure to see, the effects of coconut fibre on the flexural strength of composites were very limited, only when the coconut fibre content reached 0.4 vol.%, the flexural strength of specimen was enhanced. However, the deflection of composites with coconut fibers were greatly larger than that with no coconut fibers. This meant that coconut fibres on improving the toughness of composites were very effective.

$$y = \begin{cases} a_1 + k_1 \cdot x & (x \leq x_1) \\ y_1 + k_2 \cdot (x - x_1) & (x_1 < x \leq x_2) \\ y_2 + k_3 \cdot (x - x_2) & (x > x_2) \end{cases} \quad (1)$$

Were, $y_1 = a_1 + k_1 \cdot x_1$
 $y_2 = y_1 + k_2 \cdot (x_2 - x_1)$ (2)

3.1.2. Typical Flexural Load-Deflection Curves

For the specimens with GGBS of 10 wt.%, the flexural load-deflection curves were also linearly fitted with the same method, however, the iterative calculation was not convergent. For this case, in order to research the effects of coconut fibers on the mechanical properties of composites with GGBS of 10 wt.%, the typical flexural load-deflection curves selected from each group were plotted in Figure 6(d), which had the similar trend compared with that of composites with no GGBS. When the coconut fibre content was taken as 0.4 vol.%, the optimal flexural strength was obtained. Whatever the coconut fibre content from 0.1 to 0.5 vol.%, the flexural toughness of composites were obviously increased.

3.2. Flexural Strength

In terms of mechanics of materials, the flexural strengths of composites can be obtained from the flexural peak load. Figure 7(a) presents the flexural strengths of the foam concrete as a function of coconut fiber content. The vertical axis on the right side

represents the corresponding deflections of the specimen. Whatever the flexural strength or deflection, all the values were obtained from the average of three samples. At the same time, the standard deviations were also plotted.

Figure 7a presents the results without GGBS. When the coconut fiber content was low (0.1 and 0.2 vol.%), the flexural strength of the foamed concrete decreased which may come from more voids created by the presence of the coconut fibers. With increasing coconut Fiber volume fraction, the flexural strength increased, especially as the content of coconut fiber reached 0.4 vol.% leading to a maximum flexural strength. When the coconut fiber content was further increased to 0.5%, the flexural strength decreased again because of fiber agglomeration. Compared with the flexural strengths, the deflections have an opposite trend. When the coconut fibers volume fraction was 0.4%, the deflection was minimum. This results from the bridging role of the coconut fiber which can create some defects and voids.

Figure 7(b) presents the results when GGBS was added. Although some differences are observed compared to samples without GGBS, the optimal coconut fiber content is still at 0.4 vol.% leading to the maximum flexural strengths of 1.54 and 1.46 MPa with or without GGBS. From the previous analysis, GGBS seems to increase the brittleness of foamed concrete as the deflection at the peak point of foam concrete with GGBS decreases with increasing coconut fiber content: from 0.061, 0.045 and 0.034 mm to 0.034, 0.011 and 0.001 mm at of 0.1, 0.2 and 0.3 vol.%, respectively. However, a synergistic effect between GGBS and coconut fiber is observed as the deflection increased from 0.015 and 0.039 mm to 0.062 and 0.062 mm when the coconut fiber volume fraction is 0.4 vol.% or 0.5 vol.%

Although the related reports on mechanical strengths of coconut fiber reinforced foam concrete are very lack, Khan et al. [40] and Awoyer et al. [41]

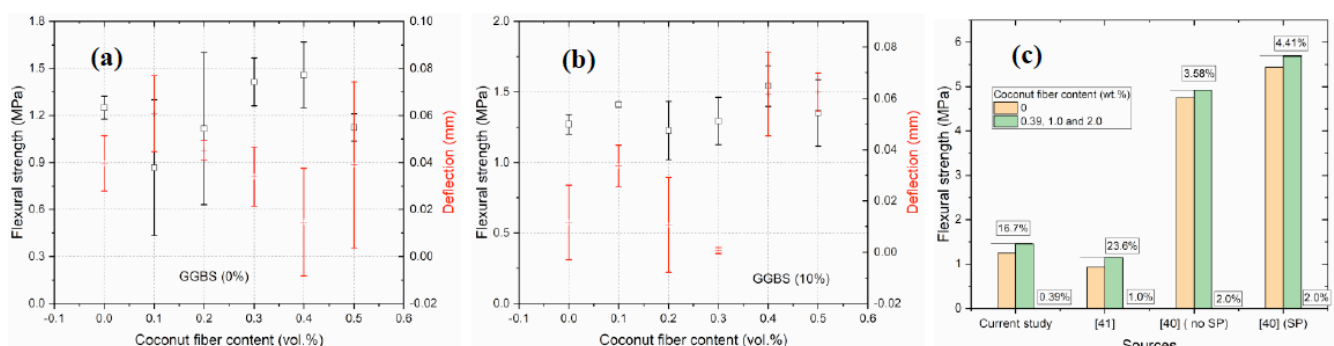


Figure 7: Flexural strength of foamed concrete as a function of coconut fiber content: (a) without GGBS and (b) with 10% GGBS, (c) comparing with reported results.

investigated the effects of coconut fiber on flexural strength of normal concrete and mortar with the same fiber length of 50 mm. Khan *et al.* used the coconut fiber content of 2.0 wt.%, and Awoyera *et al.* selected different fiber dosages of 1.0 and 1.5 wt.% on improving mechanical strength of composites. For the latter, the optimal coconut fiber content was 1.0 wt.%. To compare the effects of coconut fiber on flexural strength of cement based composites, the related results are plotted in Figure 7(c). For the reference [40], the effect of super plasticizer is also discussed. From the figure to see, when coconut fibers were added into the matrix, it can enhance the flexural strength of composites, however, the improvement to the flexural strength of composites for each case was very limited. With the coconut fiber content of 0.39, 1.0 and 2.0 wt.%, the flexural strength of composites only increased 16.7, 23.6, 3.58 and 4.41% (with SP of 0.5 wt.% to the cement)

3.3. Flexural Toughness

Coconut fiber has a higher tensile strength and elongation (Table 4) than the neat foamed concrete and this is why their presence can improve their toughness. In order to evaluate the toughness, several methods exist, such as the energy method (JCI flexural toughness), energy ratio method (ACI 544 committee flexural toughness), ASTM C1018 standard, and DBV method (Germany standard).

The *Standard test methods for fiber reinforced concrete* introduces the flexural toughness ratio (R_e) to evaluate the flexural toughness of composites as [53]:

$$R_e = \frac{f_e}{f_{cr}} \quad (3)$$

where f_e is the equivalent flexural strength (MPa), and f_{cr} is the flexural strength at the initial crack of fiber reinforced concrete calculated as:

$$f_{cr} = \frac{F_{cr}L}{bh^2} \quad (4)$$

$$f_e = \frac{\Omega_k L}{bh^2 \delta_k} \quad (5)$$

where F_{cr} is the load with the initial crack of fiber reinforced concrete. Ω_k is the area under load-deflection curve with a mid-span of $L/150$ (N·m), and δ_k is the deflection with a mid-span of $L/150$ (mm). L is the span of the beam, while b and h are the width and height of the beam cross-section, respectively. The main point of this method is that the initial crack is difficult to determine.

The *Steel fiber reinforced concrete* (JG/T 472-2015) standard introduces the concepts of initial flexural toughness ratio and flexural toughness ratio [54]. The former can be expressed as:

$$R_{e,p} = \frac{f_{e,p}}{f_{fm}} \quad (6)$$

$$f_{e,p} = \frac{\Omega_p L}{bh^2 \delta_p} \quad (7)$$

$R_{e,p}$ is the initial flexural toughness ratio, while $f_{e,p}$ and f_{fm} are the equivalent initial flexural strength and flexural strength of steel fiber reinforced concrete, respectively. Ω_p is the area (N·m) under the load-deflection curve with a mid-span of δ_p , where δ_p is the deflection at mid-span (mm). The flexural toughness ratio ($R_{e,p}$) can be expressed as:

$$R_{e,k} = \frac{f_{e,k}}{f_{fm}} \quad (8)$$

where $f_{e,k}$ is the equivalent flexural strength with a mid-span of δ_k . δ_k is the deflection at a mid-span of L/k , where k can be taken as 500, 300, 250, 200 or 150.

$$f_{e,k} = \frac{\Omega_{p,k} L}{bh^2 \delta_{p,k}} \quad (9)$$

$$\delta_{p,k} = \delta_k - \delta_p \quad (10)$$

where $\Omega_{p,k}$ is the area (N·m) under the load-deflection curve with a mid-span of $\delta_{p,k}$. $\delta_{p,k}$ is the increment between δ_p and δ_k (mm).

In our study, the initial flexural toughness ratio ($R_{e,p}$) and flexural toughness ratio ($R_{e,k}$) were selected to evaluate the flexural toughness of foamed concrete. Without GGBS, the relationships between the initial flexural toughness ratio and coconut fibers content are plotted in Figure 8(a). The initial flexural toughness ratio is marked in red, blue or pink color representing sample #1, 2 or 3. For the three samples, the average initial flexural toughness ratio is also plotted in black color. The results show that the initial flexural toughness ratio did not significantly changed at low coconut fiber content (0.1 and 0.2 vol.%), but increasing the concentration led to increased initial flexural toughness ratio, especially for a coconut fiber content of 0.4 vol.%. When GGBS was added, slight differences were observed in Figure 8b. For the neat foamed concrete, the initial flexural toughness ratio reached a maximum of 0.96. When the coconut fibres increased from 0.1 to 0.5 vol.%, the initial flexural toughness ratios were 0.64, 0.86, 0.015, 0.61 and 0.59.

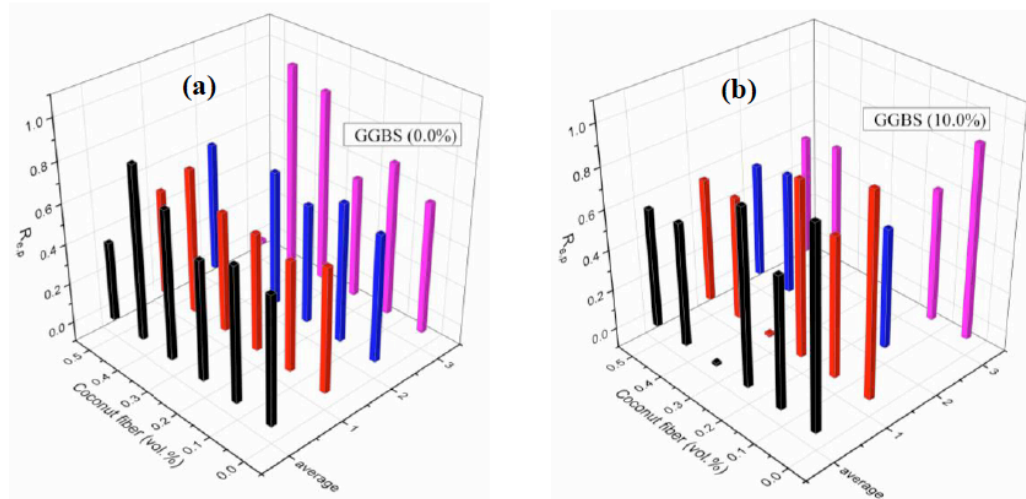


Figure 8: Relationship between the initial flexural toughness ratio and coconut fiber volume fraction with different GGBS content: (a) 0.0 wt.% and (b) 10.0 wt.%.

Compared with the neat foamed concrete without GGBS (Figure 8a), it can be seen that before the peak load, GGBS increased both the flexural strength (2%) and initial flexural toughness (54%).

After reaching the peak load, the cracks inside the specimens developed rapidly. But the presence of coconut fibers substantially improved the flexural toughness of the foamed concrete. By taking $k = 500$ in Equ. (6), this gives $L/k = 0.6$ mm and the flexural toughness ratios are also obtained without GGBS or not. Without GGBS, when the coconut fiber content was 0.5 wt.%, the flexural toughness ratio was 0.46, which is 53% higher for the neat foamed concrete (0.30). With 10% GGBS, the maximum flexural toughness ratio occurred at 0.3% of coconut fiber reaching a flexural toughness ratio of 0.49, which is 63% higher than the neat foamed concrete (0.30). similarly, the flexural toughness ratios of the foamed concrete for a mid-span deflection of 1.0, 1.2, 1.5, and

2.0 mm can be gotten. It is easy to see that the deflection of the mid-span increases with coconut fiber content. Without GGBS, the optimal coconut fiber content for the flexural toughness ratio was 0.5 vol.% (Figure 9) and the corresponding flexural toughness ratios were 0.41, 0.39, 0.43, and 0.38, respectively. These values are higher than those of the neat foamed concrete (0.16, 0.12, 0.19, and 0.09, respectively). However, when 10% GGBS was added, the optimal coconut fiber content was decreased to 0.3 vol.% and the related flexural toughness ratios are 0.42, 0.40, 0.44, and 0.37 respectively, which are also much higher than those of the neat foamed concrete (0.17, 0.13, 0.20, and 0.10, respectively).

3.4. Local axial strains

In terms of load-deflection curves for the foamed concrete with coconut fiber and GGBS, both the flexural strength and toughness can be obtained. For

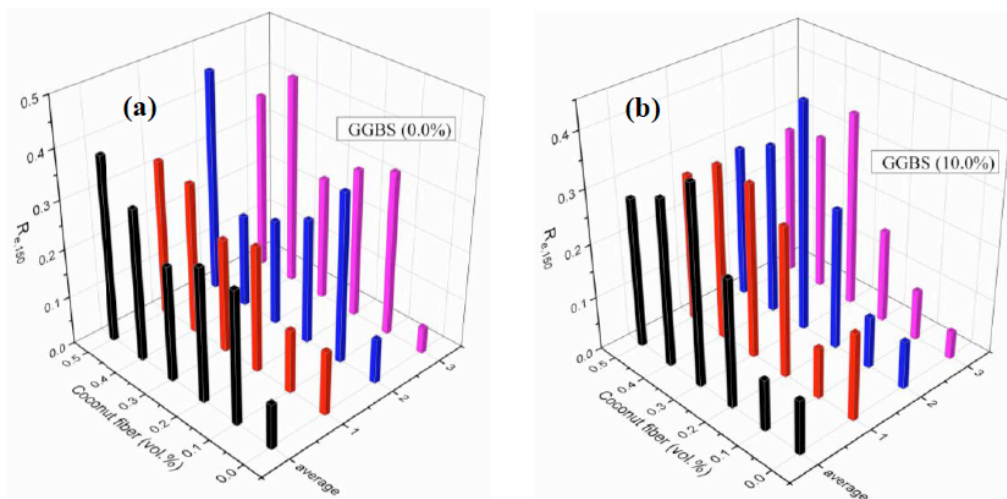


Figure 9: Relationship between the flexural toughness ratio ($L/k = 2.0$ mm) and the coconut fiber volume fraction with different GGBS content: (a) 0.0 wt.% and (b) 10.0 wt.%.

the four-point bending test, the middle part of the beam produces pure bending deformation which included axial tension or compression, while the part between the loading and support point is under axial and shear deformation. The load-deflection curves reflect the overall bearing capacity of the specimen. However, strain gauges can locally measure the strains at specific locations and get more information.

In this study, four strain gauges were installed on the top or bottom of the each specimen to measure the longitudinal or transverse strains (Figure 4). Without coconut fiber, the longitudinal strains of the three specimens are plotted in Figure 10(a), with increasing external load, both the tensile and compressive strains increased. It can be seen that GGBS increased the beam stiffness and the axial strains without GGBS are higher than those with 10.0 wt.% GGBS for a fixed external load. This indicates that foamed concrete with GGBS have lower axial deformation compared to samples without GGBS, another confirmation that GGBS makes the foamed composites more brittle.

In order to determine the effect of the transverse strains, the concept of the flexural Poisson ratio was introduced [55]. With increasing external load, the axial and transverse strains both changed and the Poisson ratio was not constant. To more conveniently compare the flexural strains, the axial and transverse strains were obtained from the average of the final measured ten values of strains. The Poisson ratios were obtained from three samples and the average are plotted in Figure 10(b). From the average values, when GGBS was added in the matrix, the Poisson ratio increased from 0.31 to 0.45. In this case, GGBS led to increased transverse strains, but lower longitudinal strains.

Figure 11(a) presents the axial strains of the foamed concrete with 0.1% coconut fiber. Although the experimental data show some scattered, the coconut fibers still efficiently enhanced the ductility; *i.e.* higher strains can be measured. Compared with the neat foamed concrete, samples without GGBS have higher strain for the same external load. This phenomenon was more obvious for sample #2. The tensile strains are higher than the compressive strains for the three

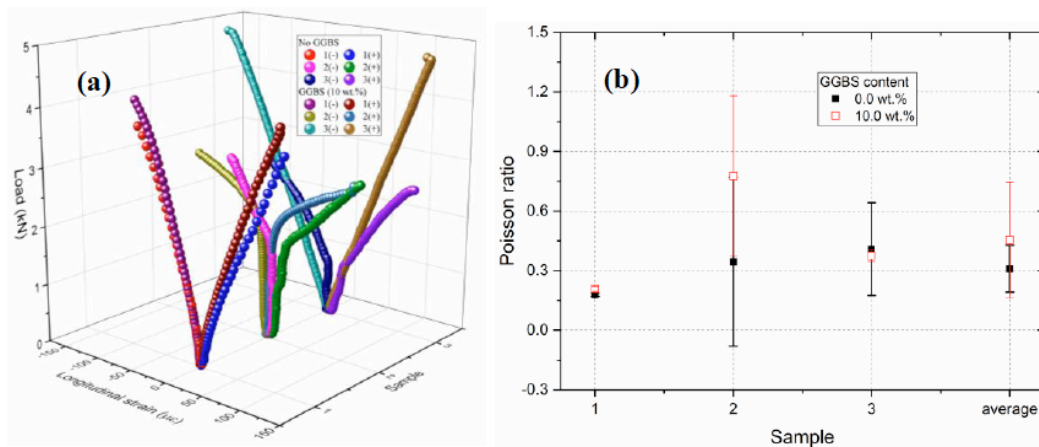


Figure 10: Strains at the top and bottom of the pure bending part for foamed concrete without coconut fiber: (a) longitudinal strains and (b) Poisson ratios.

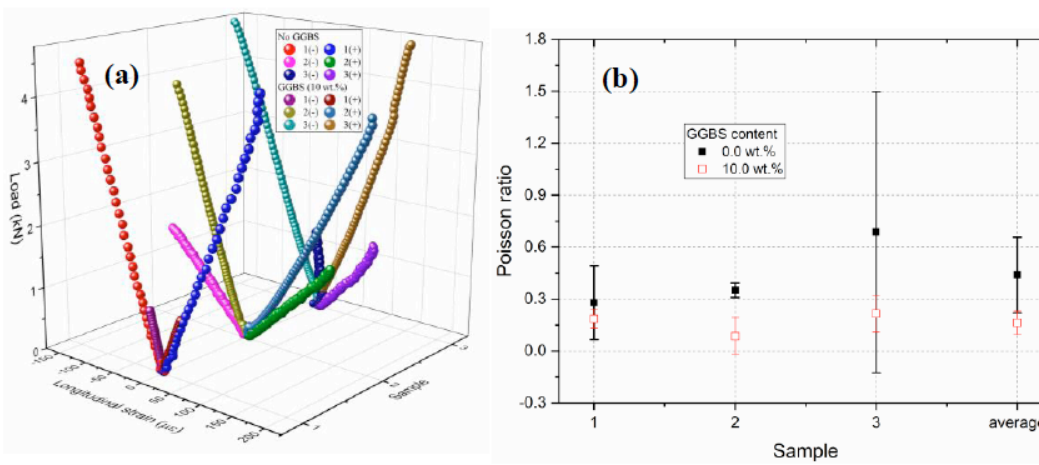


Figure 11: Strains at the top and bottom of the pure bending part for foamed concrete with 0.1 vol.% coconut fiber: (a) longitudinal strains and (b) Poisson ratios.

samples, but it shows that the specimen have an asymmetric deformation, which may be caused by the initial flexural deformation; *i.e.* before the load was applied on the specimen, it already had an initial flexural deformation due to other factors such as the weight of the specimen. This was also observed in Figure 10. Initial flexural deformation increased the tensile strain of the bottom of the specimen and decreased the corresponding compressive strain on the top. Similarly, Figure 11(b) presents the flexural Poisson ratios for the foamed concrete including the average Poisson ratios. Compared with the neat foam concrete, when coconut fibers are added, the average Poisson ratio without GGBS was larger than that with 10% GGBS. This confirms again that the hybrid system of coconut fibers with GGBS can achieve higher longitudinal strains than that of foamed concrete with coconut fibers alone.

The longitudinal strains of the foamed concrete with coconut fiber contents of 0.2, 0.3, 0.4, and 0.5 vol.% are also obtained. With increasing volume fraction of coconut fiber, the ductility increased. Because of the bridging effect of the coconut fibers, higher axial strains were measured. At 0.5% coconut fiber, the longitudinal strain value even exceeded 400 $\mu\epsilon$. Whatever the coconut fibers content, the presence of GGBS enhanced the brittleness of the foamed concrete (lower ductility).

To compare the transverse strains, the flexural Poisson ratios of the foamed concrete with different coconut fiber contents are calculated. The experimental data are similar with those of foamed concrete with 0.1% coconut fiber. From the three samples of each group, the average Poisson ratios were obtained. The presence of GGBS again decreased the Poisson ratios compared to samples without GGBS, in which the increasing axial strains trends were more obvious. When the coconut fiber content was taken as 0.2, 0.3, 0.4, and 0.5 vol.%, the

flexural Poisson ratios of the foamed concrete with 10% GGBS are 0.18, 0.15, 0.15, and 0.13 respectively, which are lower than those of the foamed concrete without GGBS (0.40, 0.26, 0.20, and 0.17). In all cases, the standard errors are reported. In general, the average Poisson ratios obtained for the foamed concrete with GGBS have slightly lower standard errors than those without GGBS. This is an indication that the samples are homogeneous.

3.5. Strain Energy Density

From the load-strain results and mechanics of materials theory, the stress-strain curves at the top and bottom of the midspan of the beam are obtained. To compare the effects of coconut fibers on the energy absorbing of composites, the strain energy densities at the compressive and tensile parts of foam concrete are calculated. The related results are plotted in Figure 12. From the Figure 12(a) to see, when the coconut fiber content exceeds 0.2 vol.%, the strain energy densities have a significant increasing especially, with the volume fraction of 0.4%, the strain energy density at the tensile location reaches 367.7 J/m^3 , which increases 472.7% compare that of the plain foam concrete. Figure 12(b) has similar results when 10 wt.% cement was replaced by GGBS. In this case, with the coconut fibers content of 0.0, and 0.4 wt.%, the corresponding strain energy densities are 80.0 and 375.6 J/m^3 . In general, it is very obvious that coconut fiber can efficiently improve the ductility of foam concrete. At the same time, the tensile energy densities are higher than compressive strain energy densities when the coconut fiber content is larger than 0.2 vol.%, which may be resulted from the initial load.

3.6. Micro-Mechanism

As for any composite, the mechanical properties of foamed concrete are not only determined by the intrinsic properties of each component, but also by the

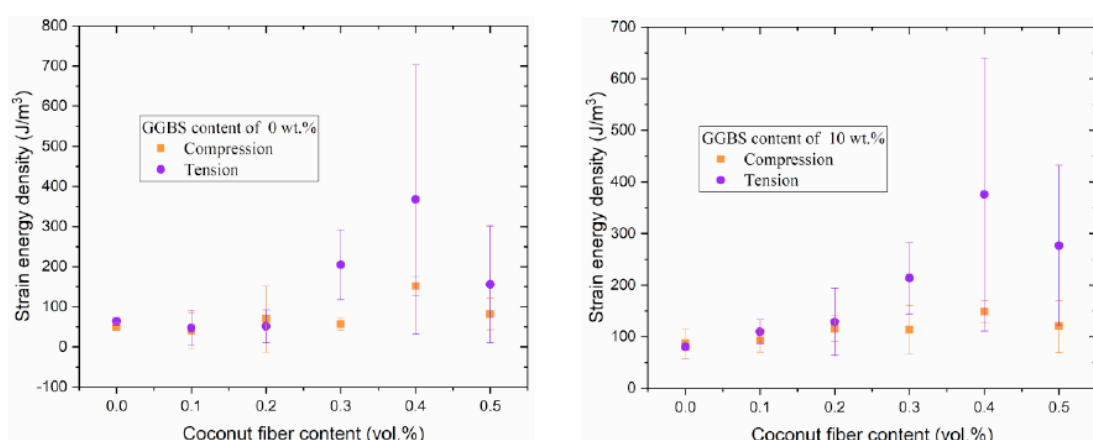


Figure 12: Strain energy density vs coconut fiber volume fraction with GGBS content of (a) 0% and (b) 10 wt.%.

micro-structure. To investigate the strengthening and toughening mechanism of foamed concrete, scanning electron microscopy (SEM) was used to analyze the samples from broken specimens. The samples are pasted on the conductive adhesive to spray with gold before being characterized.

Figure 13(a) shows the SEM image of a coconut fiber revealing that the surface was rough and covered with some impurities. The SEM image of a neat foamed concrete is presented in Figure 13(b) where voids and micro-cracks are easy to see. The closed pores come from the bubbles within the specimen. Figure 13(c) and (d) report typical SEM images of coconut fiber reinforced foamed concrete. They revealed that the coconut fibers were bonded within the cement matrix or pulled out from the matrix, which confirms that the coconut fibers were able to enhance the flexural strength and increased the ductility of foamed concrete. Similarly, the SEM images of foamed concrete with GGBS alone and the hybrid system of coconut fibers with GGBS are presented in Figure 13(e) and (f), respectively. From these figures, the size of the bubbles decreased, which may be the result from the presence of both coconut fibers and GGBS limiting their growth (volume steric hinderance). However, voids and micro cracks are still obvious, which can weaken the sample integrity and decrease the mechanical properties of foamed concrete.

4. CONCLUSIONS

With their lightweight and multi-functionality, foamed concrete is now more widely used in different civil engineering applications. However, due to the generation of several opened or closed pores within the matrix, the mechanical strength and toughness of foamed concrete can be significantly weakened. To reduce environmental pollution and develop more sustainable materials, an industrial waste residue (ground granulated blast furnace slag, GGBS) was used to partially replace the cement. Furthermore, to enhance the mechanical strength and toughness of the foamed concrete, a biobased and renewable fiber (coconut) was added due to its bridging effect and improve the mechanical performance. Based on the results obtained for the range of parameters investigated, the main conclusions for this work are as follows:

1. Before the peak loads of the load-deflection curves, there were limited deflections and the brittleness of the foamed composite was very obvious as the curves exhibited a nonlinear behavior. But when the load exceeded the peak value, the load decreased rapidly at the beginning, and then gradually flattened out. From the piecewise linear fitting curves, coconut fibres have significant effects on increasing the deflections of the beams.

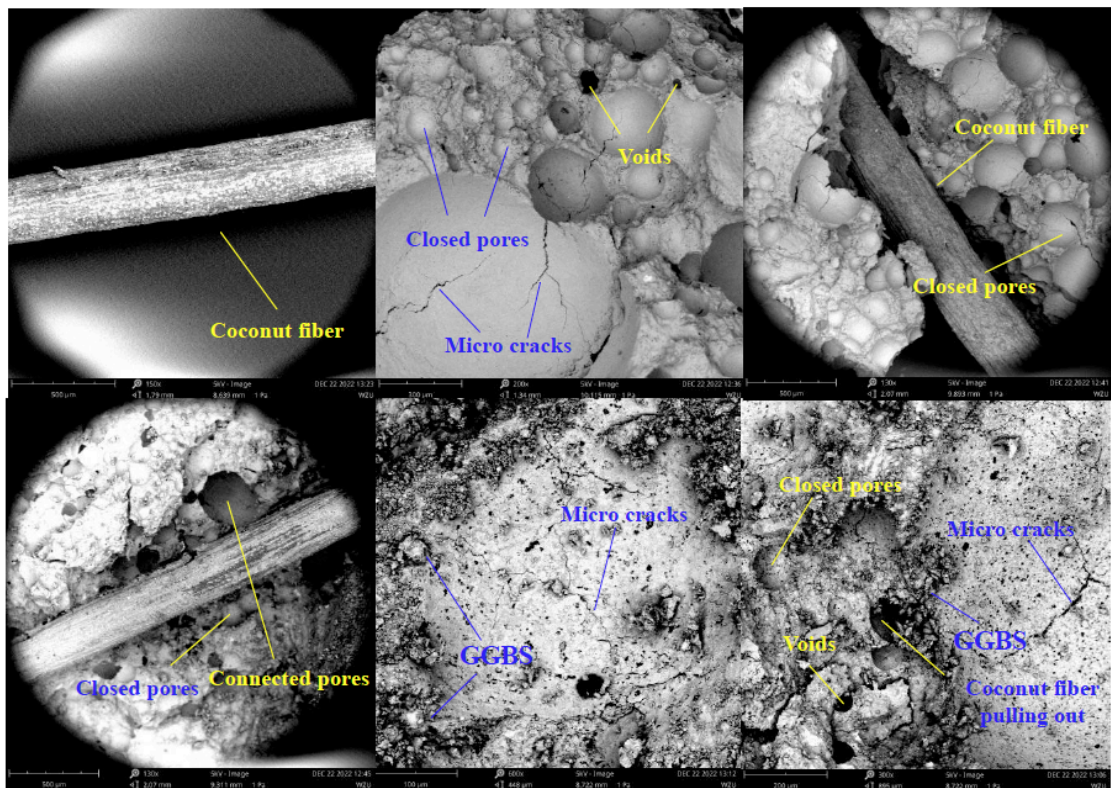


Figure 13: SEM images of the samples analyzed: (a) coconut fiber, (b) neat foamed concrete, (c) and (d) coconut fiber reinforced foamed concrete; (e) foamed concrete with GGBS, and (f) foamed concrete with coconut fiber and GGBS.

2. When the cement was partially replaced by GGBS, the flexural strengths of foamed concrete had no significant change. If coconut fibers were not added, GGBS led to more brittle samples. It was observed that the deflection (0.0117 mm) at the peak value (4.24 kN) of foamed concrete was lower than that (0.0397 mm) of the neat foamed concrete. However, when coconut fibers were added, a hybrid system with GGBS was generated with positive synergy, especially when the coconut fiber volume fraction was set at 0.4 and 0.5%. In these cases, the foamed concrete showed much larger deflections of 0.062 and 0.062 mm at the peak value of 5.14 and 4.50 kN.

3. Due to their higher tensile strength and elongation, coconut fibers can efficiently improve the flexural strength and toughness of foamed concrete. For the former, the optimal coconut fiber content was 0.4 vol.%. As GGBS was added or not, the flexural strength of foamed concrete increased by 22% or 17%. For the latter, the optimal coconut fiber content was 0.3 vol.% with 10% GGBS. The flexural toughness ratio increased by 265% when k was taken as 150. On the other hand, without GGBS, the optimal coconut fiber content was 0.5 vol.% and the flexural toughness ratio increased more (314%) for the same k value. In terms of flexural strength improvement, coconut fiber addition was more efficient to improve the flexural toughness of foamed concrete.

4. The strain gauges glued in the pure bending part of the beam were able to measure the axial and transverse strains of each specimen. For the plain foam concrete with or without GGBS, the maximum axial strains were less than $150 \mu\epsilon$, and the presence of coconut fibers can highly increase the measured strains. For example, at 0.4% coconut fiber, the maximum tensile strain reached $742 \mu\epsilon$. In this case, if the strain energy densities were calculated, the strain energy obtained from the foam concrete with the coconut fiber content of 0.4 vol.% can increase 472.7% than that from the plain foam concrete. This confirmed that coconut fibers were able to improve the ductility of foamed concrete.

5. From the SEM images, a large number of closed pores were produced, which can reduce the weight of foamed concrete (design density of 1250 kg/m^3) and increase the insulation performance. However, several connected or closed pores reduced the mechanical properties of these composites. This is why coconut fiber addition was used to partially recover some of these losses. In particular, the flexural strength and toughness was highly improved due to the bridging effect. Nevertheless, the bubbles sizes were found to decrease with increasing coconut fiber addition to limit the voids/defects in the foams.

ACKNOWLEDGEMENTS

This study was supported by the National Natural Science Foundation of China (Grant Number: 51568009), Natural Science Foundation of Zhejiang Province (Grant Number: LY18E080028) and Science and Technology plan Project of Wenzhou, China (Grant Number: S20190001, S20220005).

DECLARATIONS

Conflict of Interest

We declare that we do not have any commercial or associative interest that represents a conflict of interest in connection with the work submitted.

Ethical Approval

This article does not contain any studies with human participants or animals performed by any of the authors.

REFERENCES

- [1] R.T. Kou, M.Z. Guo, Y.Y. Shi, M.F. Mei, L.H. Jiang, H.Q. Chu, Y.Z. Zhang, H.Q. Shen, L.K. Xue, Sound-insulation and photocatalytic foamed concrete prepared with dredged sediment, *Journal of Cleaner Production* 356 (2022). <https://doi.org/10.1016/j.jclepro.2022.131902>
- [2] Z.A. Al-Absi, M.I.M. Hafizal, M. Ismail, Innovative PCM-incorporated foamed concrete panels for walls? exterior cladding: An experimental assessment in real-weather conditions, *Energ Buildings* 288 (2023). <https://doi.org/10.1016/j.enbuild.2023.113003>
- [3] O. Gencel, A. Sari, G. Kaplan, A. Ustaoglu, G. Hekimoglu, O.Y. Bayraktar, T. Ozbakkaloglu, Properties of eco-friendly foam concrete containing PCM impregnated rice husk ash for thermal management of buildings, *J Build Eng* 58 (2022). <https://doi.org/10.1016/j.jobe.2022.104961>
- [4] Y.H.M. Amran, N. Farzadnia, A.A.A. Ali, Properties and applications of foamed concrete; a review, *Constr Build Mater* 101 (2015) 990-1005. <https://doi.org/10.1016/j.conbuildmat.2015.10.112>
- [5] L.L. Guan, Y.G. Chen, D.B. Wu, Y.F. Deng, Foamed concrete utilizing excavated soil and fly ash for urban underground space backfilling: Physical properties, mechanical properties, and microstructure, *Tunn Undergr Sp Tech* 134 (2023). <https://doi.org/10.1016/j.tust.2023.104995>
- [6] C.X. Zhang, X.J. Tan, H.M. Tian, W.Z. Chen, Lateral compression and energy absorption of foamed concrete-filled polyethylene circular pipe as yielding layer for high geo-stress soft rock tunnels, *Int J Min Sci Techno* 32(5) (2022) 1087-1096. <https://doi.org/10.1016/j.ijmst.2022.08.011>
- [7] C. Rudolph, J. Valore, Cellular concrete part 1 compositions and methods of preparation, *ACI Mater J* 50(5) (1954) 24. <https://doi.org/10.14359/11794>
- [8] C. Rudolph, J. Valore, Cellular concrete part 2 physical properties, *ACI Mater J* 50(6) (1954) 20. <https://doi.org/10.14359/11795>
- [9] K. Ramamurthy, E.K.K. Nambiar, G.I.S. Ranjani, A classification of studies on properties of foam concrete, *Cement Concrete Comp* 31(6) (2009) 388-396. <https://doi.org/10.1016/j.cemconcomp.2009.04.006>
- [10] C. Liu, Y.L. Xiong, Y.N. Chen, L.T. Jia, L. Ma, Z.C. Deng, Z.B. Wang, C. Chen, N. Bantia, Y.M. Zhang, Effect of sulphoaluminate cement on fresh and hardened properties of

- [1] 3D printing foamed concrete, Compos Part B-Eng 232 (2022).
<https://doi.org/10.1016/j.compositesb.2022.109619>
- [2] M.P. Liu, Z.K. Liu, K. Wang, C.Y. Ma, H.B. Zhang, P.Z. Zhuang, Strength and deformation performances of silt-based foamed concrete under triaxial shear loading, J Build Eng 60 (2022).
<https://doi.org/10.1016/j.jobe.2022.105237>
- [3] J.Y. Shi, Y.C. Liu, H.J. Xu, Y.M. Peng, Q. Yuan, J.L. Gao, The roles of cenosphere in ultra-lightweight foamed geopolymers concrete (UFGC), Ceram Int 48(9) (2022) 12884-12896.
<https://doi.org/10.1016/j.ceramint.2022.01.161>
- [4] J.T. Dang, S.B. Zhao, G.L. Chen, X.X. Cao, J.L. Yang, Effect of polyethylene powder and heating treatment on the microstructure and hardened properties of foam concrete, J Build Eng 50 (2022).
<https://doi.org/10.1016/j.jobe.2022.104143>
- [5] K. Pasupathy, S. Ramakrishnan, J. Sanjayan, Enhancing the properties of foam concrete 3D printing using porous aggregates, Cement Concrete Comp 133 (2022).
<https://doi.org/10.1016/j.cemconcomp.2022.104687>
- [6] O. Gencel, B. Balci, O.Y. Bayraktar, M. Nodehi, A. Sari, G. Kaplan, G. Hekimog, A. Gholampour, A. Benli, T. Ozbakkaloglu, The effect of limestone and bottom ash sand with recycled fine aggregate in foam concrete, J Build Eng 54 (2022).
<https://doi.org/10.1016/j.jobe.2022.104689>
- [7] M.A.O. Mydin, M.N.M. Nawi, R. Omar, M.A. Khadimallah, I.M. Ali, R. Deraman, The use of inorganic ferrous-ferric oxide nanoparticles to improve fresh and durability properties of foamed concrete, Chemosphere 317 (2023).
<https://doi.org/10.1016/j.chemosphere.2022.137661>
- [8] C. Liu, Y.N. Chen, Y.L. Xiong, L.T. Jia, L. Ma, X.G. Wang, C. Chen, N. Banthia, Y.M. Zhang, Influence of HPMC and SF on buildability of 3D printing foam concrete: From water state and flocculation point of view, Compos Part B-Eng 242 (2022).
<https://doi.org/10.1016/j.compositesb.2022.110075>
- [9] K. Selja, I.S.R. Gandhi, Comprehensive investigation into the effect of the newly developed natural foaming agents and water to solids ratio on foam concrete behaviour, J Build Eng 58 (2022).
<https://doi.org/10.1016/j.jobe.2022.105042>
- [10] Y.L. Xiong, C. Zhang, C. Chen, Y.M. Zhang, Effect of superabsorbent polymer on the foam-stability of foamed concrete, Cement Concrete Comp 127 (2022).
<https://doi.org/10.1016/j.cemconcomp.2021.104398>
- [11] N.P. Tran, T.N. Nguyen, T.D. Ngo, P.K. Le, T.A. Le, Strategic progress in foam stabilisation towards high-performance foam concrete for building sustainability: A state-of-the-art review, Journal of Cleaner Production 375 (2022).
<https://doi.org/10.1016/j.jclepro.2022.133939>
- [12] S.L. Zhang, X.Q. Qi, S.Y. Guo, L. Zhang, J. Ren, A systematic research on foamed concrete: The effects of foam content, fly ash, slag, silica fume and water-to-binder ratio, Constr Build Mater 339 (2020).
<https://doi.org/10.1016/j.conbuildmat.2022.127683>
- [13] M.G. Li, H.B. Tan, X.Y. He, S.W. Jian, G.Y. Li, J.J. Zhang, X.F. Deng, X.L. Lin, Enhancement in compressive strength of foamed concrete by ultra-fine slag, Cement Concrete Comp 138 (2023).
<https://doi.org/10.1016/j.cemconcomp.2023.104954>
- [14] O.H. Oren, A. Gholampour, O. Gencel, T. Ozbakkaloglu, Physical and mechanical properties of foam concretes containing granulated blast furnace slag as fine aggregate, Constr Build Mater 238 (2020).
<https://doi.org/10.1016/j.conbuildmat.2019.117774>
- [15] K.H. Yang, K.H. Lee, J.K. Song, M.H. Gong, Properties and sustainability of alkali-activated slag foamed concrete, Journal of Cleaner Production 68 (2014) 226-233.
<https://doi.org/10.1016/j.jclepro.2013.12.068>
- [16] Y.F. Hao, G.Z. Yang, K.K. Liang, Development of fly ash and slag based high-strength alkali-activated foam concrete, Cement Concrete Comp 128 (2022).
<https://doi.org/10.1016/j.cemconcomp.2022.104447>
- [17] J. He, Q. Gao, X.F. Song, X.L. Bu, J.H. He, Effect of foaming agent on physical and mechanical properties of alkali-activated slag foamed concrete, Constr Build Mater 226 (2019) 280-287.
<https://doi.org/10.1016/j.conbuildmat.2019.07.302>
- [18] H.Z. Zhang, Y.C. He, C. Wang, Y.H. Guan, Z. Ge, R.J. Sun, Y.F. Ling, B. Savija, Statistical mixture design for carbide residue activated blast furnace slag foamed lightweight concrete, Constr Build Mater 342 (2022).
<https://doi.org/10.1016/j.conbuildmat.2022.127840>
- [19] D. Falliano, D. De Domenico, G. Ricciardi, E. Gugliandolo, Improving the flexural capacity of extrudable foamed concrete with glass-fiber bi-directional grid reinforcement: An experimental study, Compos Struct 209 (2019) 45-59.
<https://doi.org/10.1016/j.compstruct.2018.10.092>
- [20] D. Falliano, D. De Domenico, G. Ricciardi, E. Gugliandolo, Compressive and flexural strength of fiber-reinforced foamed concrete: Effect of fiber content, curing conditions and dry density, Constr Build Mater 198 (2019) 479-493.
<https://doi.org/10.1016/j.conbuildmat.2018.11.197>
- [21] O. Gencel, S.M.S. Kazmi, M.J. Munir, G. Kaplan, O.Y. Bayraktar, D.O. Yarar, A. Karimpour, M.R. Ahmad, Influence of bottom ash and polypropylene fibers on the physico-mechanical, durability and thermal performance of foam concrete: An experimental investigation, Constr Build Mater 306 (2021).
<https://doi.org/10.1016/j.conbuildmat.2021.124887>
- [22] D. Falliano, S. Parmigiani, D. Suarez-Riera, G.A. Ferro, L. Restuccia, Stability, flexural behavior and compressive strength of ultra-lightweight fiber-reinforced foamed concrete with dry density lower than 100 kg/m³, J Build Eng 51 (2022).
<https://doi.org/10.1016/j.jobe.2022.104329>
- [23] R. Tang, Q.S. Wei, K. Zhang, S. Jiang, Z.M. Shen, Y.X. Zhang, C.W.K. Chow, Preparation and performance analysis of recycled PET fiber reinforced recycled foamed concrete, J Build Eng 57 (2022).
<https://doi.org/10.1016/j.jobe.2022.104948>
- [24] O. Gencel, M. Nodehi, O.Y. Bayraktar, G. Kaplan, A. Benli, A. Gholampour, T. Ozbakkaloglu, Basalt fiber-reinforced foam concrete containing silica fume: An experimental study, Constr Build Mater 326 (2022).
<https://doi.org/10.1016/j.conbuildmat.2022.126861>
- [25] M. Mastali, P. Kinnunen, H. Isomoisio, M. Karhu, M. Ilikainen, Mechanical and acoustic properties of fiber-reinforced alkali-activated slag foam concretes containing lightweight structural aggregates, Constr Build Mater 187 (2018) 371-381.
<https://doi.org/10.1016/j.conbuildmat.2018.07.228>
- [26] O. Gencel, O.Y. Bayraktar, G. Kaplan, A. Benli, G. Martinez-Barrera, W. Brostow, M. Tek, B. Bodur, Characteristics of hemp fibre reinforced foam concretes with fly ash and Taguchi optimization, Constr Build Mater 294 (2021).
<https://doi.org/10.1016/j.conbuildmat.2021.123607>
- [27] J. Huang, G.X. Tian, P.Y. Huang, Z.B. Chen, Flexural Performance of Sisal Fiber Reinforced Foamed Concrete under Static and Fatigue Loading, Materials 13(14) (2020).
<https://doi.org/10.3390/ma13143098>
- [28] J. Huang, D. Rodrigue, Stiffness Behavior of Sisal Fiber Reinforced Foam Concrete under Flexural Loading, J Nat Fibers 19(15) (2022) 12251-12267.
<https://doi.org/10.1080/15440478.2022.2054896>
- [29] B. Raj, D. Sathyan, M.K. Madhavan, A. Raj, Mechanical and durability properties of hybrid fiber reinforced foam concrete, Constr Build Mater 245 (2020).
<https://doi.org/10.1016/j.conbuildmat.2020.118373>
- [30] S.H.A. Shah, M.T. Amir, B. Ali, M.H. El Ouni, Mechanical performance and environmental impact of normal strength concrete incorporating various levels of coconut fiber and recycled aggregates, Environ Sci Pollut R 29(55) (2022) 83636-83651.
<https://doi.org/10.1007/s11356-022-21608-w>

- [40] M. Khan, M. Ali, Effect of super plasticizer on the properties of medium strength concrete prepared with coconut fiber, *Constr Build Mater* 182 (2018) 703-715.
<https://doi.org/10.1016/j.conbuildmat.2018.06.150>
- [41] P.O. Awoyera, O.L. Odutuga, J.U. Effiong, A.D.S. Sarmiento, S.J. Mortazavi, J.W. Hu, Development of Fibre-Reinforced Cementitious Mortar with Mineral Wool and Coconut Fibre, *Materials* 15(13) (2022).
<https://doi.org/10.3390/ma15134520>
- [42] M. Khan, M. Ali, Improvement in concrete behavior with fly ash, silica-fume and coconut fibres, *Constr Build Mater* 203 (2019) 174-187.
<https://doi.org/10.1016/j.conbuildmat.2019.01.103>
- [43] C.L. Pereira, H. Savastano, J. Paya, S.F. Santos, M.V. Borrachero, J. Monzo, L. Soriano, Use of highly reactive rice husk ash in the production of cement matrix reinforced with green coconut fiber, *Industrial Crops and Products* 49 (2013) 88-96.
<https://doi.org/10.1016/j.indcrop.2013.04.038>
- [44] M. Amaguana, L. Guaman, N.B.Y. Gomez, M. Khorami, M. Calvo, J. Albuja-Sanchez, Test Method for Studying the Shrinkage Effect under Controlled Environmental Conditions for Concrete Reinforced with Coconut Fibres, *Materials* 16(8) (2023).
<https://doi.org/10.3390/ma16083247>
- [45] M. Ramli, W.H. Kwan, N.F. Abas, Strength and durability of coconut-fiber-reinforced concrete in aggressive environments, *Constr Build Mater* 38 (2013) 554-566.
<https://doi.org/10.1016/j.conbuildmat.2012.09.002>
- [46] M. Ali, A. Liu, H. Sou, N. Chouw, Mechanical and dynamic properties of coconut fibre reinforced concrete, *Constr Build Mater* 30 (2012) 814-825.
<https://doi.org/10.1016/j.conbuildmat.2011.12.068>
- [47] W.J. Wang, N. Chouw, The behaviour of coconut fibre reinforced concrete (CFRC) under impact loading, *Constr Build Mater* 134 (2017) 452-461.
<https://doi.org/10.1016/j.conbuildmat.2016.12.092>
- [48] H.Y. Bui, D. Levacher, M. Boutouil, N. Sebaibi, Effects of Wetting and Drying Cycles on Microstructure Change and Mechanical Properties of Coconut Fibre-Reinforced Mortar, *J Compos Sci* 6(4) (2022).
<https://doi.org/10.3390/jcs6040102>
- [49] M. Ali, X.Y. Li, N. Chouw, Experimental investigations on bond strength between coconut fibre and concrete, *Mater Design* 44 (2013) 596-605.
<https://doi.org/10.1016/j.matdes.2012.08.038>
- [50] Z. Tang, Z. Li, J. Hua, S. Lu, L. Chi, Enhancing the damping properties of cement mortar by pretreating coconut fibers for weakened interfaces, *Journal of Cleaner Production* 379 (2022).
<https://doi.org/10.1016/j.jclepro.2022.134662>
- [51] W. Ahmad, S.H. Farooq, M. Usman, M. Khan, A. Ahmad, F. Aslam, R. Alyousef, H. Alabduljabbar, M. Sufian, Effect of Coconut Fiber Length and Content on Properties of High Strength Concrete, *Materials* 13(5) (2020).
<https://doi.org/10.3390/ma13051075>
- [52] J. Huang, S.C. Qiu, D. Rodrigue, Parameters estimation and fatigue life prediction of sisal fibre reinforced foam concrete, *J Mater Res Technol* 20 (2022) 381-396.
<https://doi.org/10.1016/j.jmrt.2022.07.096>
- [53] C.C.A.f.E.C.S. CECS13., In: Standard test methods for fiber reinforced concrete. China Plan. Press; (2009).
- [54] C. Mimistry of housing and urban-rural development, Steel fiber reinforced concrete, 2015.
- [55] J. Huang, K. Xiao, D. Rodrigue, Flexural creep of multi-wall carbon nanotube reinforced cement based composites under high stress level, *Journal of Materials Research and Technology* 24 (2023) 9866-9883.
<https://doi.org/10.1016/j.jmrt.2023.05.206>

<https://doi.org/10.66000/2819-828X.2025.01.01>

© 2025 Huang et al.

This is an open-access article licensed under the terms of the Creative Commons Attribution License (<http://creativecommons.org/licenses/by/4.0/>), which permits unrestricted use, distribution, and reproduction in any medium, provided the work is properly cited.